Published OnlineFirst February 23, 2011; DOI:10.1158/1078-0432.CCR-10-2008

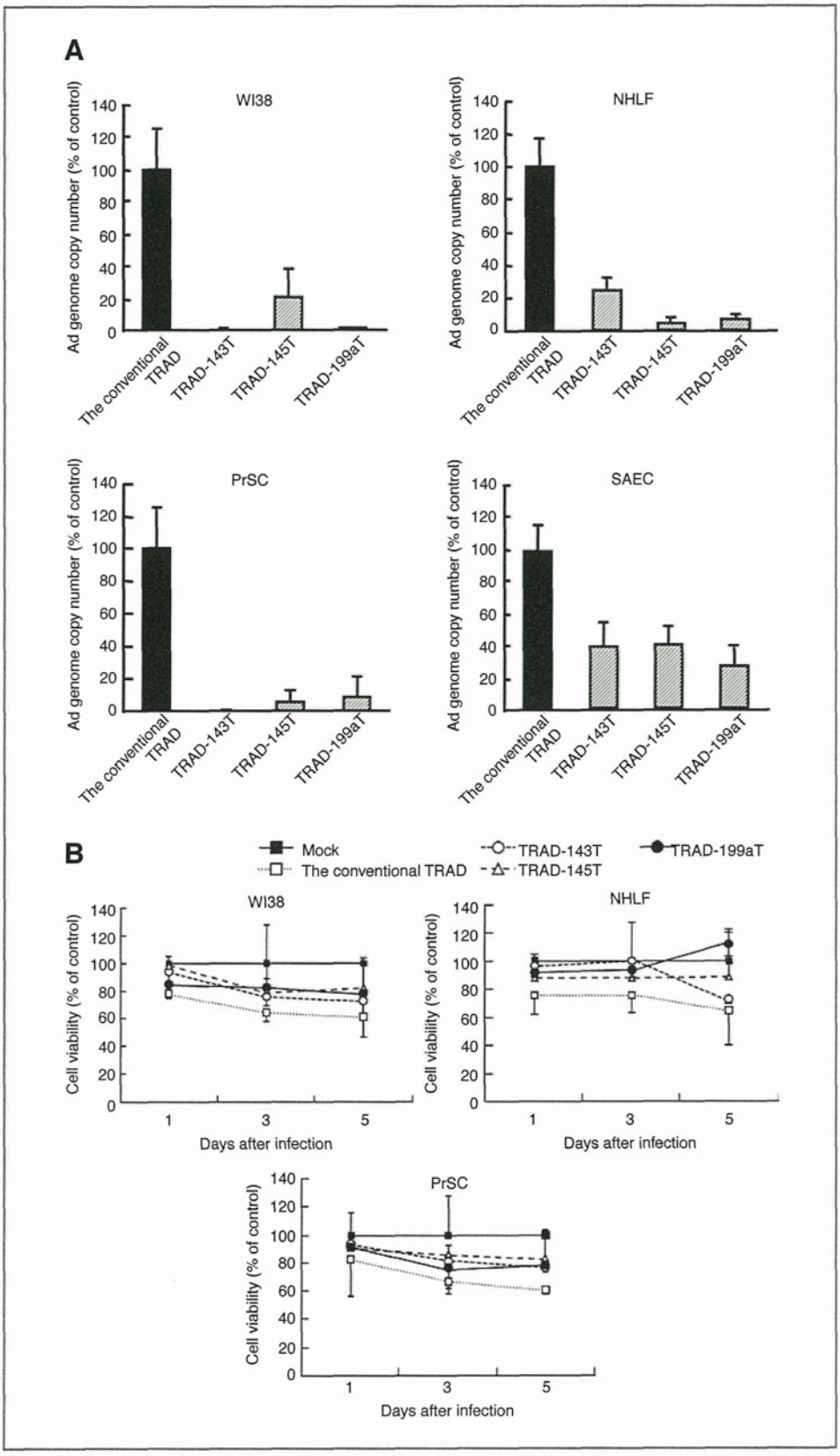

Figure 4. Reduced replication of TRADs in normal human cells by insertion of the miRNA complementary sequences. A, the viral genome copy numbers of TRADs in normal cells. The cells were infected with the TRADs at an MOI of 10 for 2 hours. Five days after infection, the viral genome copy numbers were determined by real-time PCR. B, time-course study of the normal human cell viabilities after infection with TRADs by Alamar blue assay. The cells were infected with the TRADs at an MOI of 10 for 2 hours. At the indicated time points, the viability of the cells was analyzed by Alamar blue assay. The data were normalized by the data of the mock-infected group. C, restoration of TRAD replication in human normal cells by 2′-*O*-methylated antisense oligonucleotides. The cells were transfected with 50 nmol/L of 2′-*O*-methylated antisense oligonucleotides for miR-143 or -199a. Twenty-four hours after transfection, the cells were infected with the TRADs at an MOI of 10, and the viral genome copy numbers were determined 5 days after infection with the TRADs. D, the E1A mRNA levels in normal human cells. The cells were infected with the TRADs at an MOI of 10 for 1.5 hours. Twenty-four hours after infection, the E1 mRNA levels were determined by real-time RT-PCR. The data was normalized by the data of the conventional TRAD group. All the data are shown as the means ± SD ($n = 3$–4). *, $P < 0.05$; **, $P < 0.005$.

Published OnlineFirst February 23, 2011; DOI:10.1158/1078-0432.CCR-10-2008

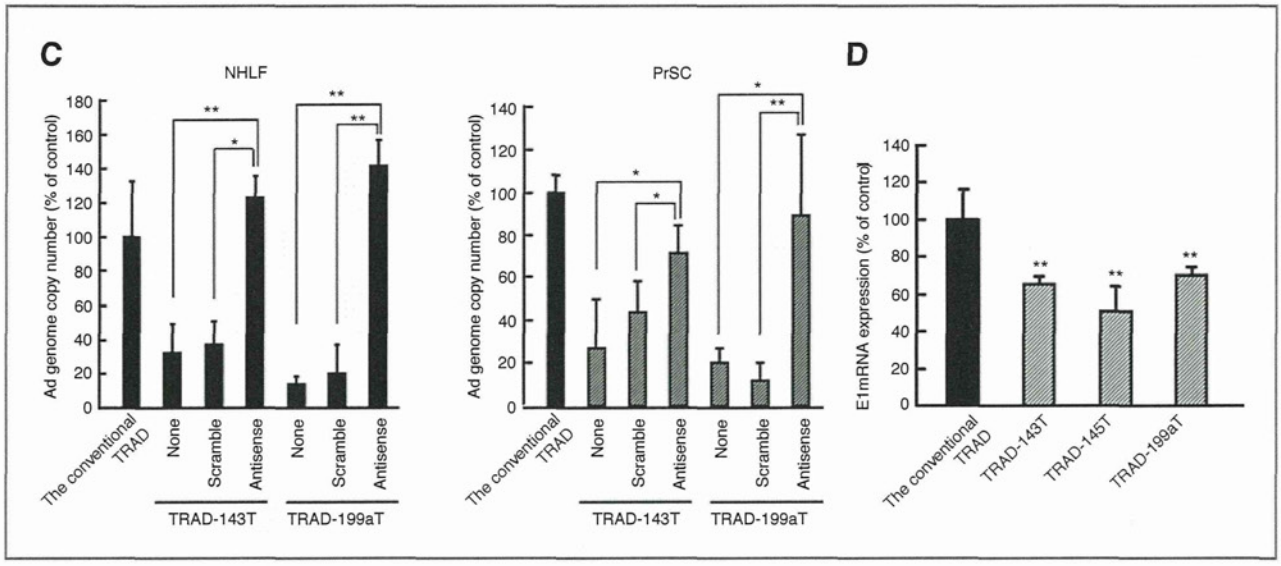

Figure 4. (*Continued*)

E1A expression by TRAD-miRT in normal cells

To determine whether incorporation of the miRNA complementary sequences into the *E1* gene expression cassette decreases the *E1* mRNA levels in normal human cells, real-time RT-PCR analysis for the E1A mRNA levels wascarried out. The E1A mRNA levels were reduced by more than 30% for TRAD-143T, -145T, and -199aT, compared with the parent TRAD, in NHLF (Fig. 4D). The reduction in the E1A mRNA levels corresponded to the suppression in replication of TRAD-miRT, indicating that miRNA-mediated reduction in the *E1* gene expression resulted in a reduced replication of TRAD-miRT.

Development of TRADs containing the complementary sequences for liver-specific miRNA

To prevent the replication of TRADs in liver hepatocytes as well as other normal cells, we incorporated not only miR-199a complementary sequences but also sequences complementary to liver-specific miR-122a into the *E1* gene expression cassette, resulting in TRAD-122a/199aT (Fig. 5A). It is well known that Ads have high hepatic tropism, leading to efficient liver accumulation even after local administration. MiR-122a was expressed approximately 100- and 20-fold more abundantly in NHep and Huh-7 cells, respectively, than in the other normal human cells and tumor cells (Fig. 5B); conversely, the other normal cells expressed more than 10-fold lower levels of miR-122a than miR-143, -145, and -199a (data not shown). Incorporation of miR-122a complementary sequences alone significantly reduced the virus genome copy number of TRAD-122aT in NHLF and NHep; however, no statistically significant decrease in the genome copy number of TRAD-122aT was found in PrSC (Fig. 5C). On the other hand, insertion of miR-199a target sequences alone was less efficient than insertion of miR-122a target sequences in NHep, probably due to the lower expression of miR-199a than miR-122a in NHep. By contrast, insertion of both miR-122a and miR-199a target sequences into the *E1* gene expression cassette efficiently reduced the replication of TRAD-122a/199aT by 10- to 50-fold in all normal cells examined. Significantly reduced replication of TRAD-122a and TRAD-122a/199aT was also found in Huh-7 cells, which are a hepatoma cell line highly expressing miR-122a and are often used as a model of hepatocytes (Supplementary Fig. S2). The incorporation of the miR-145 complementary sequences was also effective for suppressing the TRAD replication in NHep (Supplementary Fig. S3). The E1A mRNA levels were reduced for TRAD-122aT and -122a/199aT in NHep (Fig. 5D). In addition, TRAD-122a/199aT efficiently replicated in the tumor cells, resulting in efficient tumor cell lysis (Fig. 5E and F). These results indicate that replication of the TRADs in various types of normal human cells, including liver hepatocytes, is significantly reduced by insertion of the multiple target sequences to both miR-122a and -199a, without influencing the tumor cell lysis activity.

Discussion

The aim of this study was to prevent the replication of TRADs in normal human cells by incorporation of sequences complementary to miRNAs that are selectively downregulated in tumor cells, without altering the tumor cell lysis activity. Currently, there is no appropriate animal model which fully supports the *in vivo* replication of Ads and evaluation of the *in vivo* toxicity caused by oncolytic Ads, and thus it is important to be cautious in regard to oncolytic Ad-induced toxicity. To prevent the *E1* gene expression and replication of oncolytic Ads in normal cells as much as possible, an miRNA-mediated posttranscriptional detargeting system was included in TRADs, in

Published OnlineFirst February 23, 2011; DOI:10.1158/1078-0432.CCR-10-2008

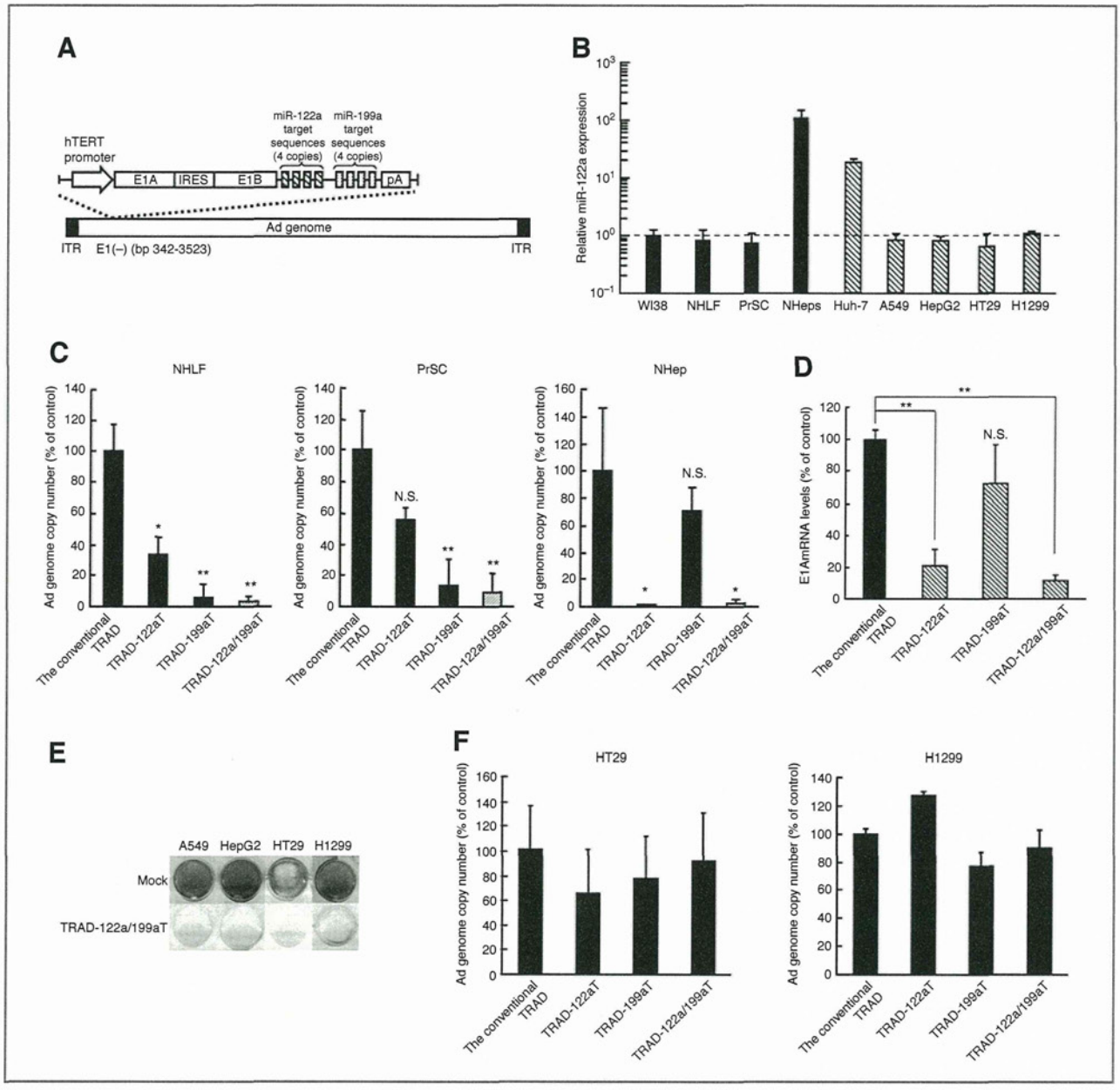

Figure 5. Tumor cell lysis activity and enhanced safety profile of TRAD-122a/199aT. A, a schematic diagram of TRAD-122a/199aT. B, miR-122a expression levels in the normal and tumor cells. C, the viral genome copy numbers of TRAD-122a/199aT in normal human cells. D, the E1A mRNA levels in NHep. E, crystal violet analysis for the cytopathic effects of TRAD-122a/199aT. The results are representative of 2 independent experiments. F, the viral genome copy numbers of TRAD-122a/199aT in tumor cells. The tumor and normal cells were infected with the TRADs at an MOI of 2 (tumor cells) or 10 (normal cells) for 2 hours. The cells were stained with crystal violet 3 days after infection. The viral genome copy numbers were determined 3 (tumor cells) or 5 days (normal cells) after infection. For determination of the E1A mRNA levels, total RNA was isolated from NHep 24 hour after infection with the TRADs at an MOI of 10, and the E1A mRNA levels were determined by real-time RT-PCR. The data was normalized by the data of the conventional TRAD group. All the data are shown as the means ± SD (n = 3–6). N.S.: not significantly different. *, $P < 0.05$; **, $P < 0.005$.

addition to the transcriptional targeting system via tumor-specific promoters.

As described above, TRAD replicates in the injected tumors and is disseminated from the injected tumors into the systemic circulation, leading to infection of distant, uninjected tumors (11, 13, 14). This property of TRAD had led to a concern that TRAD could infect normal cells over the whole body, including the hepatocytes, after dissemination from the injected tumors. It is crucial that such unexpected infection of normal cells by TRAD is prevented. Previous studies have shown that insertion of sequences complementary to liver-specific miR-122a reduced the replication of oncolytic Ads in Huh-7 cells, which are a model cell for hepatocytes (31–33). It is especially crucial

Published OnlineFirst February 23, 2011; DOI:10.1158/1078-0432.CCR-10-2008

to prevent the replication of TRAD in the liver, because Ad vectors have strong hepatotropism. However, TRAD also might infect normal cells other than hepatocytes, indicating that replication of oncolytic Ads in normal cells other than hepatocytes should also be suppressed. To prevent the replication of TRADs in other normal cells, we incorporated the sequences complementary to miR-143, -145, -199a, or let-7a, which are downregulated in the tumors and widely expressed in normal cells. The expression levels of these miRNAs in the tumor cells were lower than those in the normal cells in this study, and insertion of sequences complementary to miR-143, -145, or -199a significantly reduced the E1A mRNA levels and the replication of TRADs in the normal cells.

Overall, among the miRNA complementary sequences, the miR-199a complementary sequences appeared to be the most efficient at suppressing the replication of TRADs across all the normal cells except for hepatocytes; however, insertion of miR-199a target sequences alone failed to significantly reduce the replication of TRADs in the hepatocytes. To simultaneously prevent the replication of TRADs in various types of normal cells, including hepatocytes, we incorporated sequences complementary to miR-122a, which is abundantly expressed in hepatocytes, in addition to miR-199a target sequences. Brown and colleagues reported that a desired transgene expression pattern was achieved, depending on the miRNA expression profile, by incorporation of target sequences for 2 distinct miRNAs (34). TRAD-122aT/199aT exhibited more than 10-fold reduction in the replication in all the normal cells except for SAEC, although insertion of target sequences for miR-122a or miR-199a alone failed to suppress the replication of TRADs in either of the normal cells. Furthermore, TRAD-122aT/199aT and the parental TRAD mediated similar cytopathic efficacies in the tumor cells. These results indicate that replication of TRADs in not only hepatocytes but also other normal cells is simultaneously reduced by insertion of both miR-122a complementary sequences and sequences complementary to miRNAs highly expressed in normal cells, without altering the tumor cell lysis activity.

TRADs containing miR-122a complementary sequences are also considered to be promising for the treatment of liver cancer because miR-122a is significantly downregulated in liver cancer cells (35–37) leading to efficient replication and lytic activity of TRADs containing miR-122a complementary sequences in liver cancer cells. This study has shown that TRAD-122aT/199aT caused efficient cell lysis in a hepatocellular carcinoma cell line, HepG2 cells, while the replication of TRADs containing the miR-122a complementary sequences in normal hepatocytes, which highly express miR-122a, was significantly inhibited.

The expression levels of miRNAs are a crucial factor to suppress the gene expression by miRNAs. Brown and colleagues showed that miRNAs should be expressed at a concentration above the threshold (>100 copies/pg small RNA) to induce miRNA-regulated suppression of transgene expression (34). We were not able to precisely show the expression levels of miRNAs as the ratio of copies/pg small RNA in this study; however, comparing the miRNA levels in this study with those reported by Brown and colleagues (34), we consider that the expression levels of miR-143, -145, and -199a in the normal cells were higher than 100 copies/pg small RNA, leading to efficient suppression of the replication of TRADs.

Several studies have shown that let-7, including let-7a, is significantly downregulated in tumor cells (16, 19, 20). Edge and colleagues reported that insertion of let-7a complementary sequences into the matrix protein expression cassette of the vesicular somatitis virus (VSV) suppressed the replication of VSV in human primary fibroblast MG38 cells; on the other hand, VSV carrying let-7a target sequences efficiently replicated in A549 cells (38). However, our data showed that cancer cell lines other than HepG2 cells expressed similar or higher levels of let-7a than the normal cells. In addition, the expression levels of let-7a were more than 10-fold higher than those of the other miRNAs in the tumor cells. Abundant let-7a expression leads to a reduction in the replication of TRAD-let7aT in tumor cells. Furthermore, the members of the let-7 family, including let-7b and let-7c, have the same seed sequence, suggesting that let-7 family members other than let-7a would also contribute to the significant suppression of replication of TRAD-let7aT. These results suggest that not only expression profiles of miRNAs but also absolute amounts of miRNA expression in the cells are of great importance for miRNA-regulated gene expression.

Our data showed that the E1A mRNA levels were reduced by approximately 30% to 50% for TRAD-143T, -145T, and -199aT, compared with the conventional TRAD 24 hour after infection with the normal cells. These reduction levels in the E1A mRNA were much smaller than those in the Ad genome copy numbers at 5 days after infection; however, these reductions in the E1A mRNA levels would lead to large differences in the Ad genome copy numbers after several virus replication cycles. More than 5-fold reductions in the E1A mRNA were found for TRAD-143T, -145T, and -199aT, compared with the parental TRAD, 5 days after infection with the normal cells (data not shown).

A phase I clinical trial of the parental TRAD was conducted, and serious adverse events were not observed (3). In this study, efficient replication of the conventional TRAD in WI38 cells was found at an MOI of 10; however, the conventional TRAD did not exhibit a high level of replication at an MOI of 2. It might be unlikely that such a high titer (MOI 10) of oncolytic Ad would infect organs distal from the injection points in clinical trials; however, normal cells around the injection points might be infected with a high titer of oncolytic Ad. In addition, even though no apparent replication of TRADs is observed in normal cells after infection of TRADs, the expression of Ad proteins, including E1A and E4 proteins, affects the cellular functions via various mechanisms (39–41). This study indicates that inclusion of an miRNA-regulated *E1* gene expression system in oncolytic Ads enhances the safety of oncolytic Ads and makes it possible to increase the injection doses, leading to superior therapeutic effects.

Published OnlineFirst February 23, 2011; DOI:10.1158/1078-0432.CCR-10-2008

In summary, we developed TRADs in which the *E1* gene expression is controlled by miRNAs more highly expressed in normal cells than tumor cells. The TRADs containing the sequences complementary to miR-143, -145, or -199a exhibited reduced replication in the normal cells without altering the tumor cell lysis activity. Furthermore, incorporation of both miR-199a and miR-122a target sequences significantly suppressed the replication in all human primary cells examined, including hepatocytes. TRAD-miRT has enhanced both the safety profiles and comparable tumor cell lysis activity to the parental TRAD, suggesting that TRAD-miRT offers great potential for the treatment of tumors.

Disclosure of Potential Conflicts of Interest

Toshiyoshi Fujiwara and Hiroyuki Mizuguchi are consultants to Oncolys BioPharma, Inc. No other potential conflicts of interest were disclosed.

Acknowledgments

We thank Takako Ichinose, Koyori Yano (National Institute of Biomedical Innovation, Osaka, Japan), and Sayuri Okamoto (Graduate School of Pharmaceutical Sciences, Osaka University, Osaka, Japan) for their help.

Grant Support

Support was received from a grant-in-aid for Young Scientists (A) F. Sakurai from the Ministry of Education, Culture, Sports, Science, and Technology (MEXT) of Japan (F. Sakurai), and a grant from the Takeda Science Foundation (H. Mizuguchi).

The costs of publication of this article were defrayed in part by the payment of page charges. This article must therefore be hereby marked *advertisement* in accordance with 18 U.S.C. Section 1734 solely to indicate this fact.

Received July 28, 2010; revised November 18, 2010; accepted December 14, 2010; published OnlineFirst February 23, 2011.

References

1. Mathis JM, Stoff-Khalili MA, Curiel DT. Oncolytic adenoviruses—selective retargeting to tumor cells. Oncogene 2005;24:7775–91.
2. Ribacka C, Pesonen S, Hemminki A. Cancer, stem cells, and oncolytic viruses. Ann Med 2008;40:496–505.
3. Nemunaitis J, Tong AW, Nemunaitis M, Senzer N, Phadke AP, Bedell C, et al. A phase I study of telomerase-specific replication competent oncolytic adenovirus (telomelysin) for various solid tumors. Mol Ther 2010;18:429–34.
4. Li JL, Liu HL, Zhang XR, Xu JP, Hu WK, Liang M, et al. A phase I trial of intratumoral administration of recombinant oncolytic adenovirus overexpressing HSP70 in advanced solid tumor patients. Gene Ther 2009;16:376–82.
5. Freytag SO, Movsas B, Aref I, Stricker H, Peabody J, Pegg J, et al. Phase I trial of replication-competent adenovirus-mediated suicide gene therapy combined with IMRT for prostate cancer. Mol Ther 2007;15:1016–23.
6. Li Y, Yu DC, Chen Y, Amin P, Zhang H, Nguyen N, et al. A hepatocellular carcinoma-specific adenovirus variant, CV890, eliminates distant human liver tumors in combination with doxorubicin. Cancer Res 2001;61:6428–36.
7. Rodriguez R, Schuur ER, Lim HY, Henderson GA, Simons JW, Henderson DR. Prostate attenuated replication competent adenovirus (ARCA) CN706: a selective cytotoxic for prostate-specific antigen-positive prostate cancer cells. Cancer Res 1997;57:2559–63.
8. Matsubara S, Wada Y, Gardner TA, Egawa M, Park MS, Hsieh CL, et al. A conditional replication-competent adenoviral vector, Ad-OC-E1a, to cotarget prostate cancer and bone stroma in an experimental model of androgen-independent prostate cancer bone metastasis. Cancer Res 2001;61:6012–9.
9. Yamamoto M, Davydova J, Wang M, Siegal GP, Krasnykh V, Vickers SM, et al. Infectivity enhanced, cyclooxygenase-2 promoter-based conditionally replicative adenovirus for pancreatic cancer. Gastroenterology 2003;125:1203–18.
10. Kawashima T, Kagawa S, Kobayashi N, Shirakiya Y, Umeoka T, Teraishi F, et al. Telomerase-specific replication-selective virotherapy for human cancer. Clin Cancer Res 2004;10:285–92.
11. Taki M, Kagawa S, Nishizaki M, Mizuguchi H, Hayakawa T, Kyo S, et al. Enhanced oncolysis by a tropism-modified telomerase-specific replication-selective adenoviral agent OBP-405 ('Telomelysin-RGD'). Oncogene 2005;24:3130–40.
12. Watanabe T, Hioki M, Fujiwara T, Nishizaki M, Kagawa S, Taki M, et al. Histone deacetylase inhibitor FR901228 enhances the antitumor effect of telomerase-specific replication-selective adenoviral agent OBP-301 in human lung cancer cells. Exp Cell Res 2006;312:256–65.
13. Umeoka T, Kawashima T, Kagawa S, Teraishi F, Taki M, Nishizaki M, et al. Visualization of intrathoracically disseminated solid tumors in mice with optical imaging by telomerase-specific amplification of a transferred green fluorescent protein gene. Cancer Res 2004;64:6259–65.
14. Kishimoto H, Kojima T, Watanabe Y, Kagawa S, Fujiwara T, Uno F, et al. In vivo imaging of lymph node metastasis with telomerase-specific replication-selective adenovirus. Nat Med 2006;12:1213–9.
15. Hitt MM, Graham FL. Adenovirus E1A under the control of heterologous promoters: wide variation in E1A expression levels has little effect on virus replication. Virology 1990;179:667–78.
16. Takamizawa J, Konishi H, Yanagisawa K, Tomida S, Osada H, Endoh H, et al. Reduced expression of the let-7 microRNAs in human lung cancers in association with shortened postoperative survival. Cancer Res 2004;64:3753–6.
17. Michael MZ, SM OC, van Holst Pellekaan NG, Young GP, James RJ. Reduced accumulation of specific microRNAs in colorectal neoplasia. Mol Cancer Res 2003;1:882–91.
18. Slaby O, Svoboda M, Fabian P, Smerdova T, Knoflickova D, Bednarikova M, et al. Altered expression of miR-21, miR-31, miR-143 and miR-145 is related to clinicopathologic features of colorectal cancer. Oncology 2007;72:397–402.
19. Yanaihara N, Caplen N, Bowman E, Seike M, Kumamoto K, Yi M, et al. Unique microRNA molecular profiles in lung cancer diagnosis and prognosis. Cancer Cell 2006;9:189–98.
20. Johnson SM, Grosshans H, Shingara J, Byrom M, Jarvis R, Cheng A, et al. RAS is regulated by the let-7 microRNA family. Cell 2005;120:635–47.
21. Mizuguchi H, Kay MA. Efficient construction of a recombinant adenovirus vector by an improved in vitro ligation method. Hum Gene Ther 1998;9:2577–83.
22. Mizuguchi H, Kay MA. A simple method for constructing E1- and E1/E4-deleted recombinant adenoviral vectors. Hum Gene Ther 1999;10:2013–7.
23. Sakurai F, Kawabata K, Yamaguchi T, Hayakawa T, Mizuguchi H. Optimization of adenovirus serotype 35 vectors for efficient transduction in human hematopoietic progenitors: comparison of promoter activities. Gene Ther 2005;12:1424–33.
24. Maizel JV Jr, White DO, Scharff MD. The polypeptides of adenovirus. I. Evidence for multiple protein components in the virion and a comparison of types 2, 7A, and 12. Virology 1968;36:115–25.
25. Koizumi N, Kawabata K, Sakurai F, Watanabe Y, Hayakawa T, Mizuguchi H. Modified adenoviral vectors ablated for coxsackievirus-adenovirus receptor, alphav integrin, and heparan sulfate binding reduce in vivo tissue transduction and toxicity. Hum Gene Ther 2006;17:264–79.
26. Ishii-Watabe A, Uchida E, Iwata A, Nagata R, Satoh K, Fan K, et al. Detection of replication-competent adenoviruses spiked into recombinant adenovirus vector products by infectivity PCR. Mol Ther 2003;8:1009–16.

Published OnlineFirst February 23, 2011; DOI:10.1158/1078-0432.CCR-10-2008

27. Iorio MV, Visone R, Di Leva G, Donati V, Petrocca F, Casalini P, et al. MicroRNA signatures in human ovarian cancer. Cancer Res 2007;67:8699–707.
28. Mathonnet G, Fabian MR, Svitkin YV, Parsyan A, Huck L, Murata T, et al. MicroRNA inhibition of translation initiation in vitro by targeting the cap-binding complex eIF4F. Science 2007;317:1764–7.
29. Petersen CP, Bordeleau ME, Pelletier J, Sharp PA. Short RNAs repress translation after initiation in mammalian cells. Mol Cell 2006;21:533–42.
30. Pillai RS, Bhattacharyya SN, Artus CG, Zoller T, Cougot N, Basyuk E, et al. Inhibition of translational initiation by Let-7 MicroRNA in human cells. Science 2005;309:1573–6.
31. Cawood R, Chen HH, Carroll F, Bazan-Peregrino M, van Rooijen N, Seymour LW. Use of tissue-specific microRNA to control pathology of wild-type adenovirus without attenuation of its ability to kill cancer cells. PLoS Pathog 2009;5:e1000440.
32. Leja J, Nilsson B, Yu D, Gustafson E, Akerstrom G, Oberg K, et al. Double-detargeted oncolytic adenovirus shows replication arrest in liver cells and retains neuroendocrine cell killing ability. PLoS One 2010;5:e8916.
33. Ylosmaki E, Hakkarainen T, Hemminki A, Visakorpi T, Andino R, Saksela K. Generation of a conditionally replicating adenovirus based on targeted destruction of E1A mRNA by a cell type-specific MicroRNA. J Virol 2008;82:11009–15.
34. Brown BD, Gentner B, Cantore A, Colleoni S, Amendola M, Zingale A, et al. Endogenous microRNA can be broadly exploited to regulate transgene expression according to tissue, lineage and differentiation state. Nat Biotechnol 2007;25:1457–67.
35. Coulouarn C, Factor VM, Andersen JB, Durkin ME, Thorgeirsson SS. Loss of miR-122 expression in liver cancer correlates with suppression of the hepatic phenotype and gain of metastatic properties. Oncogene 2009;28:3526–36.
36. Bai S, Nasser MW, Wang B, Hsu SH, Datta J, Kutay H, et al. MicroRNA-122 inhibits tumorigenic properties of hepatocellular carcinoma cells and sensitizes these cells to sorafenib. J Biol Chem 2009;284:32015–27.
37. Gramantieri L, Ferracin M, Fornari F, Veronese A, Sabbioni S, Liu CG, et al. Cyclin G1 is a target of miR-122a, a microRNA frequently downregulated in human hepatocellular carcinoma. Cancer Res 2007;67:6092–9.
38. Edge RE, Falls TJ, Brown CW, Lichty BD, Atkins H, Bell JC. A let-7 MicroRNA-sensitive vesicular stomatitis virus demonstrates tumor-specific replication. Mol Ther 2008;16:1437–43.
39. Duerksen-Hughes P, Wold WS, Gooding LR. Adenovirus E1A renders infected cells sensitive to cytolysis by tumor necrosis factor. J Immunol 1989;143:4193–200.
40. Ramalingam R, Worgall S, Rafii S, Crystal RG. Downregulation of CXCR4 gene expression in primary human endothelial cells following infection with E1(-)E4(+) adenovirus gene transfer vectors. Mol Ther 2000;2:381–6.
41. Weitzman MD. Functions of the adenovirus E4 proteins and their impact on viral vectors. Front Biosci 2005;10:1106–17.

Cell Cycle 10:16, 2737-2741; August 15, 2011; © 2011 Landes Bioscience

Tumor-selective adenoviral-mediated GFP genetic labeling of human cancer in the live mouse reports future recurrence after resection

Hiroyuki Kishimoto,[1-3] Ryoichi Aki,[1,2] Yasuo Urata,[4] Michael Bouvet,[2] Masashi Momiyama,[1,2] Noriaki Tanaka,[3] Toshiyoshi Fujiwara[3] and Robert M. Hoffman[1,2,*]

[1]AntiCancer, Inc.; [2]Department of Surgery; University of California at San Diego; San Diego, CA USA; [3]Division of Surgical Oncology; Department of Surgery; Okayama University Graduate School of Medicine; Dentistry and Pharmaceutical Sciences; Okayama, Japan; [4]Oncolys BioPharma, Inc.; Tokyo, Japan

Key words: green fluorescent protein, adenovirus, cancer labeling, in situ, fluorescence-guided surgery, recurrence, detection

We have previously developed a telomerase-specific replicating adenovirus expressing GFP (OBP-401), which can selectively label tumors in vivo with GFP. Intraperitoneal (i.p.) injection of OBP-401 specifically labeled peritoneal tumors with GFP, enabling fluorescence visualization of the disseminated disease and real-time fluorescence surgical navigation. However, technical problems of removing all cancer cells still remain, even with fluorescence-guided surgery. In this study, we report that in vivo OBP-401 labeling of tumors with GFP before fluorescence-guided surgery reports cancer recurrence after surgery. Recurrent tumor nodules brightly expressed GFP, indicating that initial OBP-401-GFP labeling of peritoneal disease was genetically stable such that proliferating residual cancer cells still express GFP. In situ tumor labeling with a genetic reporter has important advantages over antibody and other non-genetic labeling of tumors, since residual disease remains labeled during recurrence and can be further resected under fluorescence guidance.

Introduction

Green fluorescent protein (GFP) serves as a very bright genetic reporter to detect metastatic cancer in mouse models.[1-3] Initially, cancer cells were transduced in vitro with GFP using various types of genetic vectors and then implanted in mouse models. Potential clinical application of GFP became possible when it was demonstrated that retroviruses containing GFP could label disseminated cancer in situ in mouse models.[4] Subsequently, selective in vivo GFP labeling of tumors was performed with OBP-401, a replicating adenovirus[5,6] that contains a replication cassette with the human telomerase reverse transcriptase (hTERT) promoter driving the expression of the viral *E1* genes, and the inserted *GFP* gene. Virus replication and hence *GFP* gene expression occur only in the presence of an active telomerase, i.e., in malignant tissue.[6] The OBP-401 virus was first tested by injection directly into HT-29 human colon tumors, orthotopically implanted into the rectum in BALB/c *nu/nu* mice. Subsequent para-aortic lymph node metastasis was observed by laparotomy under fluorescence.[6] We then developed a major enhancement of cancer surgical navigation in orthotopic mouse models of cancer, using in vivo selective fluorescent tumor labeling with OBP-401 GFP. Bright GFP fluorescence clearly illuminated the tumor boundaries and facilitated detection of the smallest disseminated disease lesions.[7]

Fluorescence-guided surgical navigation with tumors labeled in vivo with OAP-401 GFP was demonstrated in nude mouse models that represent difficult surgical challenges for the resection of widely disseminated cancer. HCT-116, a model of intraperitoneal disseminated human colon cancer, was labeled by virus injection into the peritoneal cavity. A549, a model of pleural dissemination of human lung cancer, was labeled by OBP-401 virus administered into the pleural cavity. Only the malignant tissue fluoresced brightly in both models. Further, we showed that OBP-401 could visualize liver metastases by tumor-specific expression of the GFP gene after portal venous or i.v. administration. Selective metastatic tumor labeling with GFP and killing by systemic administration of telomerase-dependent adenoviruses suggesting that liver metastasis is also a candidate for fluorescence-guided surgery.[8]

However, even fluorescence-guided surgery may still result in residual disease. The present report demonstrates proliferating residual disease remains stably labeled with OBP-401 GFP and is readily detected for further resection, suggesting that genetic-reporter labeling of tumors has advantages over non-genetic labeling of tumors for fluorescence-guided surgery.

Results and Discussion

Labeling peritoneal carcinomatosis with OBP-401-GFP. Peritoneal carcinomatosis was induced in the abdominal cavity of nude mice by i.p. implantation of HCT-116-RFP human colorectal cancer cells. Twelve days after implantation, 1 x 10^8 PFU

*Correspondence to: Robert M. Hoffman; Email: all@anticancer.com
Submitted: 06/01/11; Revised: 06/09/11; Accepted: 06/10/11
DOI: 10.4161/cc.10.16.16756

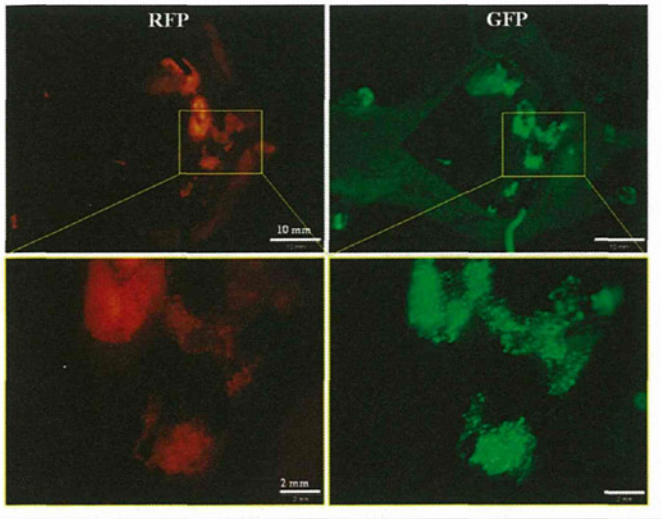

Figure 1. In situ genetic labeling of disseminated peritoneal carcinomatosis. Red fluorescence indicates HCT-116-RFP-expressing disseminated nodules (left). Peritoneal disseminated HCT116-RFP cells were labeled by GFP after i.p. injection of OBP-401 (right). Fluorescence imaging revealed co-localization of red and green fluorescence.

OBP-401 were injected intraperitoneally. Disseminated HCT-116-RFP nodules expressed GFP fluorescence induced by OBP-401 as well as the endogenous RFP fluorescence when imaged 5 d later (**Fig. 1**). RFP fluorescence was essentially coincident with that of GFP, indicating that i.p. injection of OBP-401 efficiently labeled disseminated tumors with GFP.

Stability of OBP-401-GFP expression in tumors. In order to determine stability of GFP expression in OBP-401 labeled tumors, HCT-116-RFP tumors were collected by peritoneal lavage from the abdominal cavity of mice 5 d after OBP-401 administration, put into culture in RPMI 1640 medium supplemented with 10% FBS and observed over time. Eight days after plating (13 d after viral administration), cancer cell colonies expressed both RFP and GFP (**Fig. 2**). The stability of GFP expression in OBP-401 labeled tumor cells suggests the potential of OBP-401 GFP labeling to detect recurrent tumors after attempted resection.

Fluorescence-guided resection of disseminated peritoneal tumors labeled with OBP-401 GFP. Five days after OBP-401 administration to mice with i.p. HCT-116, laparotomy was performed with the intent to remove all the intra-abdominal cancer using fluorescence-guided navigation under ketamine anesthesia (**Fig. 3A and B**). OBP-401 labeling and imaging made disseminated cancer nodules visible by GFP fluorescence, and complete resection was attempted (**Fig. 3C–E**). Tumors were efficiently resected, including those not visible under bright light, as we have previously reported in references 7 and 8.

In vivo detection of recurrent OBP-402-GFP labeled tumors after fluorescence-guided surgery. Tumors still recurred after attempted complete resection with fluorescence-guided surgery as visualized by GFP expression (**Fig. 4**). This result demonstrates that OBP-401 GFP labeling of peritoneal disseminated disease enables detection of tumor recurrence after fluorescence-guided surgery. Thus, OBP-401-GFP labeling is genetically stable and therefore proliferating residual disease continues to express GFP.

Tsien's laboratory has developed a method to label and visualize tumors during surgery using activatable cell-penetrating peptides (ACPPs), in which the fluorescently-labeled, polycationic cell-penetrating peptide (CPP) is coupled via a cleavable linker to a neutralizing peptide. Upon exposure to proteases expressed by tumors, the linker is cleaved, dissociating the inhibitory peptide and allowing the CPP to bind to and enter tumor cells. Animals whose tumors were resected with ACPPD guidance had better long-term tumor-free survival and overall survival than animals whose tumors were resected with traditional brightfield illumination only.[9]

Another approach to tumor labeling and fluorescence-guided surgery is with the use of labeled tumor-specific antibodies. A monoclonal antibody specific for CA19-9 was conjugated to a green fluorophore and delivered to tumor-bearing mice as a single intravenous (IV) dose. Intravital fluorescence imaging was used to localize metastatic pancreatic cancer in orthotopic mouse models 24 h after antibody administration. Using fluorescence imaging, the primary tumor was clearly visible at laparotomy, as were small metastases in the liver and spleen and on the peritoneum. The metastatic tumors, which were nearly impossible to see using standard brightfield imaging, demonstrated clear fluorescence under LED light excitation.[10]

We have also previously investigated the use of fluorophore-labeled anti-carcinoembryonic antigen (CEA) monoclonal antibody to aid in cancer visualization in nude mouse models of human colorectal and pancreatic cancer. Anti-CEA was conjugated with a green fluorophore. Subcutaneous, orthotopic primary and metastatic human pancreatic and colorectal tumors were easily visualized with fluorescence imaging after administration of conjugated anti-CEA. The fluorescence signal was detectable 30 min after systemic antibody delivery and remained present for 2 weeks, with minimal in vivo photobleaching after exposure to standard operating room lighting. Fluorescent anti-CEA administration improved ability to resect the labeled tumors under fluorescence guidance.[11]

Neither the ACPP nor labeled monoclonal antibodies, described above, involves genetic labeling of cancer cells, and thus recurrence would therefore not be detectable. In the present study, we selectively and efficiently labeled tumors with a genetic reporter, GFP, using a telomerase dependent adenovirus OBP-401. We demonstrated that tumors recurred after fluorescence-guided surgery and maintained GFP expression. Therefore, the detection of recurrence and future metastasis is possible with OBP-401 GFP labeling, since recurrent cancer cells stably express GFP, which is not possible with non-genetic labeling of tumors.

In clinical studies performed with OBP-401, circulating tumor cells (CTC) obtained from cancer patients were labeled with OBP-401 GFP ex vivo. OBP-401-GFP labeling greatly increased the detection of CTC.[12] Other targets for in vivo GFP labeling could include, for example, breast cancer emboli.[13] Specific labeling by GFP of cancer stem cells is also a promising approach.[14]

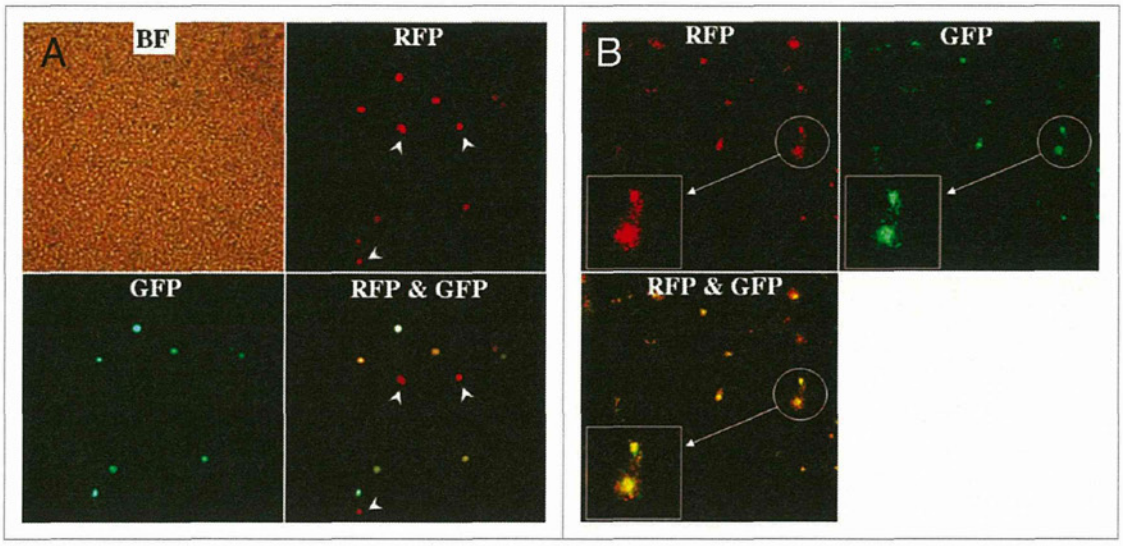

Figure 2. Genetic labeling of microscopic tumors. Cells collected by peritoneal lavage from the abdominal cavity of mice 5 d after OBP-401 treatment were plated and cultured with RPMI 1640 medium supplemented with 10% FBS. (A) Plating cells in the peritoneal lavage fluid (5 d after viral administration). Most RFP-expressing cancer cells expressed GFP fluorescence induced by OBP-401 as well, x200 magnification. White arrows: cells unlabeled with GFP. (B) 8 d after plating (i.e., 13 d after viral administration). Cancer cell colonies expressing RFP were observed in the culture dish under fluorescence microscopy. The cancer cells also expressed GFP induced by OBP-401. x40 magnification. Boxes highlight colonies indicated by white circles. Original magnification x100.

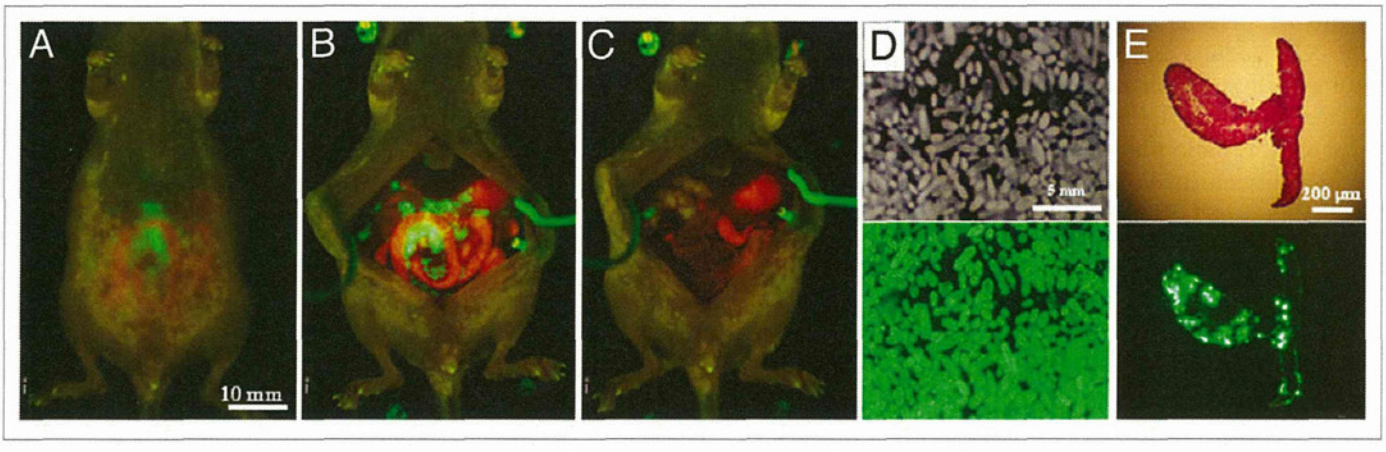

Figure 3. Fluorescence-guided resection of tumors labeled with GFP in situ. (A) Peritoneal disseminated nodules were labeled by GFP expression 5 d after OBP-401 virus administration. (B) Laparotomy was performed. (C) Disseminated nodules labeled with GFP were removed under GFP-guided surgical navigation. (D) Disseminated nodules removed under GFP-guided navigation. Top, bright field observation; bottom, fluorescent detection. (E) Section of disseminated nodules. Top, H&E section; bottom, frozen section with fluorescence detection.

Labeling of cancer stem cells is especially important, since at least some stem cells can now be imaged non-invasively.[15] The present report suggests the clinical potential of OBP-401 GFP labeling to improve the surgical outcome of cancer.

Materials and Methods

Recombinant adenovirus. Telomerase-specific replication-selective adenovirus OBP-401, containing the *GFP* gene under the control of the CMV promoter with the hTERT promoter driving the *E1A* and *E1B* genes, was constructed and produced as previously described in references 5 and 6.

Cell culture. The human colorectal cancer cell line HCT-116 was cultured in RPMI 1640 medium supplemented with 10% FBS.

Production of red fluorescent protein (RFP) retroviral vector. For RFP retrovirus production, the *Hind*III/*Not*I fragment from pDsRed2 (Clontech), containing the full-length RFP cDNA, was inserted into the *Hind*III/*Not*I site of pLNCX2 (Clontech) containing the neomycin-resistance gene. PT67, an NIH3T3-derived packaging cell line (Clontech) expressing the viral envelope, was cultured in DMEM supplemented with 10% FBS. For vector production, PT67 packaging cells, at 70% confluence, were incubated with a precipitated mixture of LipofectAMINE reagent

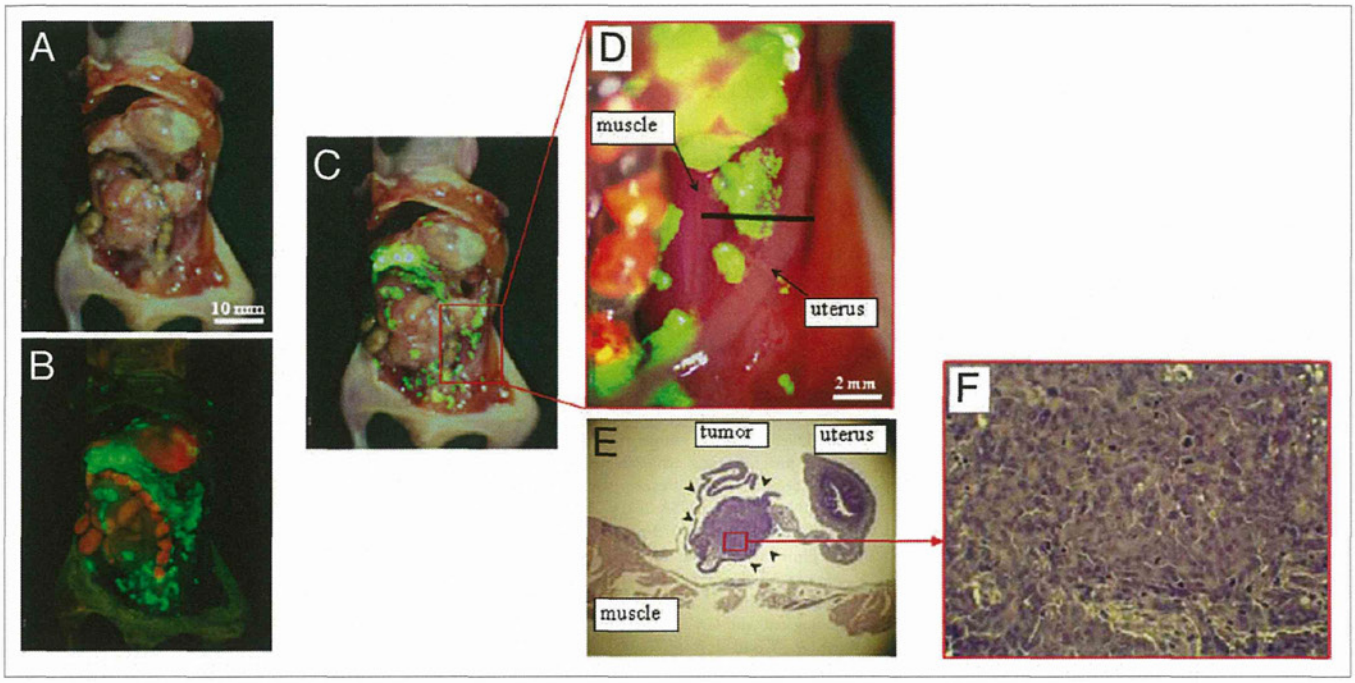

Figure 4. In vivo detection of recurrent tumors after fluorescence-guided surgery. (A) Brightfield observation several weeks after fluorescence-guided surgery of OBP-401 GFP-labeled tumors. Disseminated disease re-emerged. (B) Fluorescence observation of field observed by brightfield in (A). (C) Merge of (A and B). The red box outlines a region of (D) below. (D) Detail of the boxed region of (C). Black line indicates the direction of cross-sections. (E) Histologic sections stained with H&E showing that GFP-labeled lesions are recurrent tumor tissues (arrow heads). x40 magnification. (F) Detail of the boxed region of (E). x200 magnification.

(Life Technologies) and saturating amounts of pLNCX2-DsRed2 plasmid for 18 h. Fresh medium was replenished at this time. The cells were examined by fluorescence microscopy 48 h post-transduction. For selection of a clone producing high amounts of RFP retroviral vector (PT67-DsRed2), the cells were cultured in the presence of 200 to 1,000 μg/ml G418 (Life Technologies) for 7 d. The isolated packaging cell clone was termed PT67-DSRed2.[16]

RFP gene transduction of cancer cells. For RFP gene transduction, cancer cells were incubated with a 1:1 precipitated mixture of retroviral supernatants of PT67 cells and RPMI 1640 containing 10% FBS for 72 h. Fresh medium was replenished at this time. Tumor cells were harvested with trypsin/EDTA 72 h post-transduction and subcultured at a ratio of 1:15 into selective medium, which contained 200 μg/ml G418. To select brightly fluorescent cells, the level of G418 was increased up to 800 μg/ml in a stepwise manner. RFP-expressing cancer cells were isolated with cloning cylinders using trypsin/EDTA and were amplified by conventional culture methods in the absence of selective agent.[16]

Mice. Athymic nude mice were kept in a barrier facility under HEPA filtration and fed with autoclaved laboratory rodent diet. All animal studies were conducted in accordance with the principals and procedures outlined in the National Institute of Health Guide for the Care and Use of Laboratory Animals under Assurance Number A3873-1. All animal procedures were performed under anesthesia using s.c. administration of a ketamine mixture (10 μl ketamine HCL, 7.6 μl xylazine, 2.4 μl acepromazine maleate and 10 μl PBS).

In vivo fluorescence imaging. An Olympus OV100 Small Animal Imaging System (Olympus Corp., Tokyo, Japan) with macro and micro optics was used.[17] High-resolution images directly captured on a PC were processed and analyzed with the use of Adobe Photoshop Elements 4.0 software (Adobe).

Peritoneal carcinomatosis model with HCT-116 human colon cancer cells implanted in nude mice. Nude mice were intraperitoneally (i.p.) injected either with HCT-116 or HCT-116-RFP human colon cancer cells at a density of 3 x 10^6 in 200 μl PBS. Twelve days after tumor cell inoculation, mice were injected i.p. with OBP-401 at a dose of 1 x 10^8 PFU in 200 μl PBS. Five days after virus injection, the abdominal cavity was examined by fluorescence imaging, and mice were operated on with fluorescence guidance with the intent to resect all intra-abdominal tumor nodules under ketamine-induced anesthesia.

Collection of microscopic tumors from peritoneal lavage fluid of OBP-401 treated mice. Twelve days after nude mice were i.p. injected with HCT-116-RFP, 1 x 10^8 PFU OBP-401 were injected intraperitoneally. Five days after virus injection, mice were instilled with 8 ml PBS intraperitoneally. The abdomen was gently massaged and the peritoneal fluid was carefully aspirated using a 22-gauge needle. Approximately 6 ml peritoneal lavage fluid (PLF) were obtained from most mice. After filtering the PLF with a 40 μm cell strainer (BD, Franklin Lakes, NJ) in order to collect only microscopic tumors and/or cancer cells in the abdominal cavity, 3 ml of PLF were cultured on 6-well tissue culture plates. After incubation for 1 h, supernatants were carefully aspirated and 3 ml RPMI 1640 medium, containing 10% FBS,